R-PEAK DETECTION USING WAVELET TRANSFORMS TECHNIQUE

Skander BENSEGUENI[1], Abdelhak BENNIA[2]

This paper presents a technique based on wavelet transforms to analyze the electrocardiogram signal (ECG) for the detection of the R peaks. We locate the QRS complexes of this signal using the dyadic wavelet transform (DyWT) and detect the R peaks using the direction change mark method (DCM). Applied on the ECG signal database MIT-BIH, the algorithm that we present gave good results for detecting the R waves with a rate of 99.91%, a sensitivity of 99.95 % and a positive predictivity of 99.96 %.

Keywords: ECG, R-peak, wavelet transforms

1. Introduction

The QRS complex is the largest wave of the ECG signal, its identification permits the calculation of the heart rate and the determination of the ST segment for proper diagnosis of some cardio-myopathies, in addition to the classification of waves as normal or not such as premature ventricular contraction (PVC), supraventricular contraction (SVC), ventricular late potentials (VLP), atrial premature contraction (APC), right bundle branch block (RBBB), left bundle branch block (LBBB), etc. [1]. This is the reason why several algorithms have been developed to analyze the signal in an automatic way. However, the nonlinearity, the non stationarity of the ECG signal, and the noise (artifacts) that affects it represent the major problems for the design of effective treatment techniques. Artifacts are defined as deflections of the ECG that are due to influences other than cardiac activity of the heart. There are several types of artifacts [2]:

1) Motion artifacts: the result of these movements for the ECG leads to a shift of the baseline that appears much more in PR segment, shifting the isoelectric line of zero amplitude. It represents a low frequency disturbance of approximately 0.1 Hz.

[1] Doctoral student, Department of Electronic, Université Frères Mentouri, Constantine, Algeria, e-mail: benskandix@gmail.com

[2] Professor, Department of Electronic, Université Frères Mentouri, Constantine, Algeria, e-mail: abdelhak.bennia@laposte.net

2) Baseline distortion: appears in shifts of the isoelectric line due to cable movements and the frequency of such noise is in the range of 0.1 to 10 Hz.
3) Sector artifacts: which are due to the device voltage source and are high frequency noises (50 or 60 Hz).
4) Muscle artifacts: this type of noises is due to muscle contractions. We can note that the RR intervals for these artifacts are very regular.

In recent years, many QRS detectors of ECG signals have been developed to facilitate the diagnosis of the human heart. These algorithms are based primarily on the use of two main steps: the first step is the preprocessing stage, where the signal undergoes filtering operations to eliminate or minimize the noise and improve and make possible the detection, while the second step is the detection of QRS complexes that can be performed by different processing such as transformations, thresholding and the implementation of a decision rule for the R peaks (Fig. 1).

We may well find ECG signal analysis algorithms based on the derivative and on the differentiation for the detection [2-4], where a candidate R peak is defined as one of the points within the derivative slopes interval exceeding a predefined threshold. A method that uses digital filters was implemented in [5] for the baseline distortions and high frequency elimination. Nonlinear transformations were used in [6-8] by squaring operations and moving windows for QRS complexes detection. Linear prediction based methods were applied in [9,10], the first one uses the prediction coefficients of the discrete cosine transform in order to estimate ECG signals by performing a singular value decomposition while the second one uses features extraction. Methods using neural networks gave good results in terms of true wave detection but they take a very long time in the learning and the training steps [11-12]. An ECG analysis method by filter banks was also used in [13]. Other studies have used wavelet transforms [14-21]. The wavelet transform is a good technique for time-frequency analysis which decomposes the signal into elementary blocks well localized in time and frequency. The work that we will perform, will focus on the implementation of the wavelet transform for ECG signal analysis in order to filter it by eliminating the baseline deviations and the high frequency noises, and then detect the R peaks.

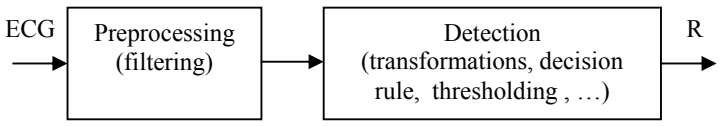

Fig. 1. Structure of the R-peak detectors

2. Theory

2.1. Wavelet transform. The continuous wavelet transform is given according to the mother wavelet function $\psi(t)$ as follows:

$$C(a,b) = \int_{-\infty}^{\infty} x(t)\,\psi_{a,b}(t)\mathrm{d}t \tag{1}$$

$$\psi_{a,b}(t) = (1/\sqrt{a})\,\psi((t-b)/a) \tag{2}$$

Where $\psi_{a,b}$ is the dilation function, a is the scale factor and b is the translation parameter. If we let:

$$a = 2^{-j} \text{ and } b = k\,2^{-j} \tag{3}$$

the transformation will be given by:

$$DyWT_x^{\psi}(j,k) = C_{j,k} = 2^{j/2}\int_{-\infty}^{\infty} x(t)\,\psi\left(2^j t - k\right)\mathrm{d}t \tag{4}$$

The digitalization of this transform is computed by Mallat's algorithm which represents the multiresolution approach [22]. In multiresolution analysis, a function is viewed at various levels of resolution, it gives the approximation and detail coefficients of the discrete wavelet transform by the following equations [22-24]:

$$AC_j(k) = \sum_{n=-\infty}^{\infty} h_{\varphi}(n-2k)AC_{j+1}(n) \tag{5}$$

$$DC_j(k) = \sum_{n=-\infty}^{\infty} h_{\psi}(n-2k)DC_{j+1}(n) \tag{6}$$

Where $h_{\varphi}(n)$ is the sequence of the low pass filter coefficients H_{φ} and $h_{\psi}(n)$ is the sequence of wavelet coefficients of the high pass filter H_{ψ}.

This realization of the DWT by the filter banks of the decomposition wavelet tree produces an output signal that spreads from high to low frequencies with varying degrees of bandwidth. The detail coefficients resulting from band pass filters whose center frequencies gradually decrease because of increased number of low pass filters $h_{\varphi}(n)$ which have been cascaded to the high pass filter, while the coefficient $AC_3(k)$ describing the approximation signal is obtained by cascading low pass filters only [22]. Thus, each filter has a different equivalent bandwidth (Table 1) [14].

We note from the frequency response of the wavelet transform equivalent filter that small scales reflect the high frequencies components and large scales reflect the low frequencies ones, these low and high frequencies explain the existence of noise, artifacts and other waves of the ECG signal (*P*, *T* and *U*).

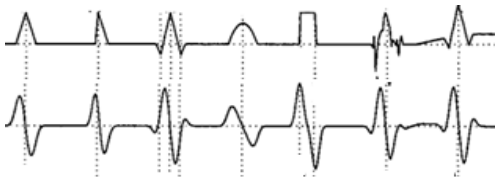

Fig. 2. The top figure shows waves of different shapes and the bottom figure shows the zero crossings of the dyadic wavelet transform DyWT for scale $j = 3$

Table 1

Equivalent filters bandwidth for different scales

Scales	Bandwidths (Hz)
2^1	62.5 to 125.0
2^2	18 to 58.5
2^3	8 to 27
2^4	4 to 13.5
2^5	2 to 6.5

From Fig. 2, we can verify that a wave corresponds to a successive positive maximum and negative minimum of its dyadic wavelet transform for different scales. The positive maximum corresponds to the descending portion and the minimum negative to the ascending portion of the wave, while its peak corresponds to the zero crossing.

2.2. Direction change mark method. A peak is also detected by the direction change mark (DCM) which is sensitive to changes in direction and therefore to the presence of peaks; it is based on the first level details signal (FLDS) [25]. The FLDS is obtained using the following procedure (Fig. 3):

1) Calculate the first approximation coefficients $AC_1(k)$ and the first detail coefficients $DC_1(k)$ of the discrete wavelet transform in order 1 of the Haar mother wavelet by the equations (5) and (6), respectively. The Haar wavelet is due to its characteristic of discontinuity and its resemblance to a step function which makes it very sensitive to changes in slopes of the original signal.
2) Then, put all the approximation coefficients $AC_1(k)$ to zero.
3) At the end, reconstruct the signal by the inverse discrete wavelet transform using the new coefficients $AC_1(k)$ (all zeros) and the coefficients $DC_1(k)$ and thus we obtain the FLDS.

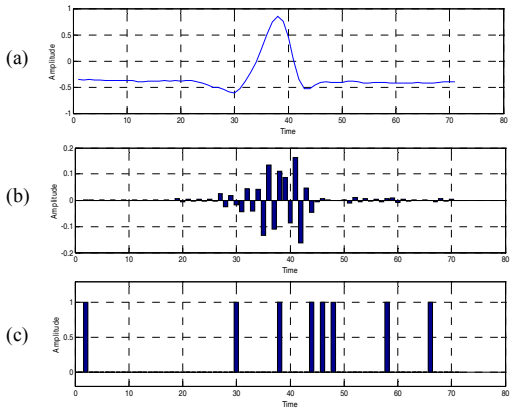

Fig. 3. The direction change mark method (a) ECG signal, (b) FLDS and (c) DCM equal to zero except at the peaks of the signal

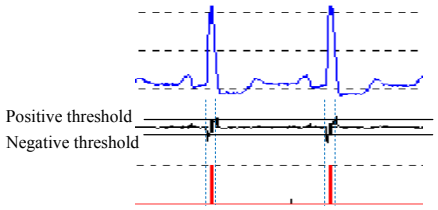

Fig. 4. In blue: ECG signal, in black: DyWT (negative minimum-positive maximum pairs) and in red: DCM which is equal to zero except at the *R*-peak

The main property of the FLDS is that the samples are of the same magnitude and alternating signs if the slope of the wave is constant, and there is a change in direction of the latter, and in the change point, two successive samples of the FLDS have the same sign. This change of direction is marked by the DCM. The DCM is a vector that has the same number of samples as the original signal. All elements of this vector are zeros except the point of changing direction, equal to one.

We used the DCM method to locate the ECG signal *R* peaks of the QRS complex. It is noted from Fig. 4 that each QRS complex is represented by at least a couple of negative minimum-positive maximum (the minimum for the positive slope and the maximum for the negative one) and the *R* peak that occurs between these two is represented by a DCM=1 for all peaks. So, we are in presence of an *R* peak if the DCM is not equal to zero.

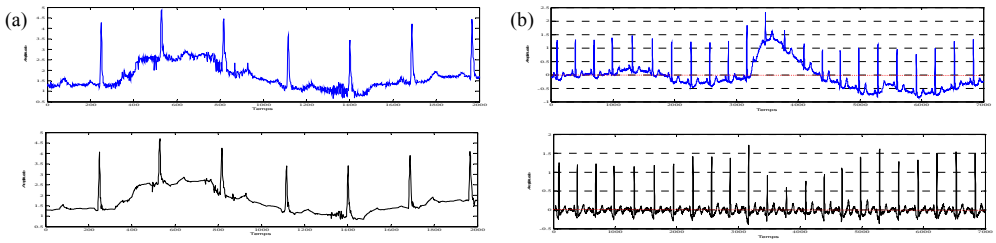

Fig. 5. (a) The high frequency filtering of one segment of 101 ECG recording from the MIT-BIH database and (b) The low frequency filtering of another segment of 101 ECG recording from the MIT-BIH database. In blue: ECG signal, in black: filtered signal and in red baseline

3. Method

3.1. ECG signal filtering. The variations in the ECG baseline are seen in frequencies around 0.1 Hz, therefore they are equivalent to large orders of the approximation coefficients of the discrete wavelet transform. This property is very important for the elimination of the baseline distortions of the ECG signal. Our filter is based on the decomposition of the signal by a discrete wavelet transform and the choice of the mother wavelet ψ which gives the best results. After a comparative study between different levels and different types of mother wavelets, the decomposition is performed in the order 6 of the approximation coefficients and Daubechies (db11) mother wavelet. The following procedure is applied for low frequency filtering (Fig. 5b):

1) Choose the type of mother wavelet.
2) Compute the discrete wavelet decomposition in the order 6 of the ECG signal using Mallat's algorithm by the introduction of the wavelet and the scaling coefficients of the approximation and detail filters respectively for the wavelet db11 in (5) and (6).
3) Setting the approximation coefficients of zero order $AC_6(k)$ to zero, and letting the other approximation coefficients $AC_j(k)$ $(1 \leq j \leq 6)$ and detail coefficients $DC_j(k)$ $(1 \leq j \leq 6)$ unchanged.
4) Rebuilding the ECG signal using the inverse discrete wavelet transform and the new coefficients, to have finally the last approximation coefficients that give the signal $x(t)$.

It was noted also that we can observe the high frequency noise of the ECG signal for low orders of detail coefficients of the discrete wavelet transform. Based on this important property, we design a nonlinear filter for the elimination of the high frequency noise. The use of nonlinear filtering is due to the limitation of linear filtering to eliminate the high frequency noise or the signal rapid

variation and keeping the signal smooth at the same time. The nonlinear filtering based on the detail coefficients of the discrete wavelet transform gives good results without altering the characteristics of the signal.

The high frequency filtering procedure is resumed in the determination of the detail coefficients by a discrete wavelet transform, and then set to zero the coefficients below a certain threshold, to finally reconstruct the filtered signal from the new coefficients using the inverse discrete wavelet transform (Fig. 5a):

1) Choose a Daubechies mother wavelet db2.
2) Compute the discrete wavelet decomposition of the noisy signal in the order 3 of the detail coefficients (6).
3) Calculate the detail coefficients threshold of the first level $DC_1(k)$. We calculate the average value μ and standard deviation σ of the absolute value of detail coefficients $DC_1(k)$ of the ECG signal discrete wavelet transform. The threshold value will be:
$$S = \sigma\sqrt{2\ln(N)} \tag{7}$$
4) All the detail coefficients of all levels ($DC_1(k)$, $DC_2(k)$, $DC_3(k)$) that are less than S will be set equal to zero, while the other coefficients will be modified to obtain new coefficients:
$$DC_{j,1\le j\le 3}Mo(k) = \begin{cases} DC_j(k) - (sign\left(DC_j(k)\right)S), if\ DC_j(k) > S \\ 0 \qquad\qquad\qquad\qquad\quad , if\ DC_j(k) \le S \end{cases} \tag{8}$$
5) Calculate the inverse discrete wavelet transform using these new coefficients in order to have the filtered signal.

3.2. QRS complexes location. Our detection method is based on the use of different types of wavelet transform properties for locating with precision QRS waves, and is described by the following.

We calculate the dyadic wavelet transform of the ECG signal $x(t)$ in (4), and then choose the level 2^3 ($j = 3$) of this transform:
$$DyWT_x^{\psi}(3,k) = C_{3,k} = 2^{-3/2}\int_{-\infty}^{\infty} x(t)\,\psi(2^{-3}(t-k))\mathrm{d}t \tag{9}$$
The choice of this scale is due to the energy distribution mostly in the QRS interval as defined by the equivalent filter of the scale 2^3 (Table 1).

We search for the dyadic wavelet transform positive maxima and negative minima to locate the various waves of the ECG signal. It may be noted that the DyWT of a QRS, which focuses on the location, has the largest amplitude in comparison with other ECG characteristic waves. This encourages us to use thresholds large enough so that we can detect the DyWT waves of the QRS, by proceeding as follows:

1) Choose a positive threshold $S_p(k)$ and a negative threshold $S_n(k)$. The first is used to determine the probable positive maximum $m_p(k)$ and the second for the probable minimum negative $m_n(k)$ of the QRS wavelet transform.
2) Check if the DyWT calculated by (13) exceeds the thresholds, if

$$\begin{cases} C_{3,k} > S_p(k), & so: m_p(k) = C_{3,k} \text{ is a probable maximum} \\ C_{3,k} < S_n(k), & so: m_n(k) = C_{3,k} \text{ is a probable minimum} \end{cases} \quad (10)$$

Note that $M_p(k)$ and $M_n(k)$ are the maximum of $m_p(k)$ and the minimum of $m_n(k)$ for the same pair of negative minimum-positive maximum, respectively.

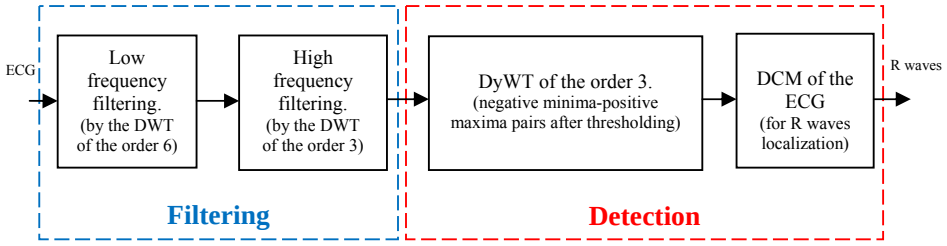

Fig. 6. The block diagram of the *R*-peak detector

Table 2.

R-peak detection results of our wavelets-based algorithm of fifteen MIT-BIH database records

Records	Beats Number	FP	FN	Failed Detection (beats)	Failed Detection (%)
100	2273	0	0	0	0
101	1865	0	1	1	0.05
102	2187	0	2	2	0.09
103	2084	0	0	0	0
112	2539	5	0	5	0.20
113	1795	0	2	2	0.11
115	1953	0	0	0	0
118	2275	0	0	0	0
122	2476	0	0	0	0
123	1518	0	3	3	0.20
215	3363	0	2	2	0.06
219	2154	0	7	7	0.32
220	2048	0	0	0	0
230	2256	7	0	7	0.31
234	2753	0	0	0	0
Total Number	33539	12	17	29	0.09

3) Make the adjustment of thresholds S_p and S_n using the following procedure:
If $C_{3,k} > 2\ S_p(k)$, then

otherwise

We will have the positive thresholds:

and if $C_{3,k} < 2\ S_n(k)$, then

else

We will have at the end the negative thresholds:

This step allowed us the determination of the negative minima-positive maxima pairs of possible QRS complexes transforms.

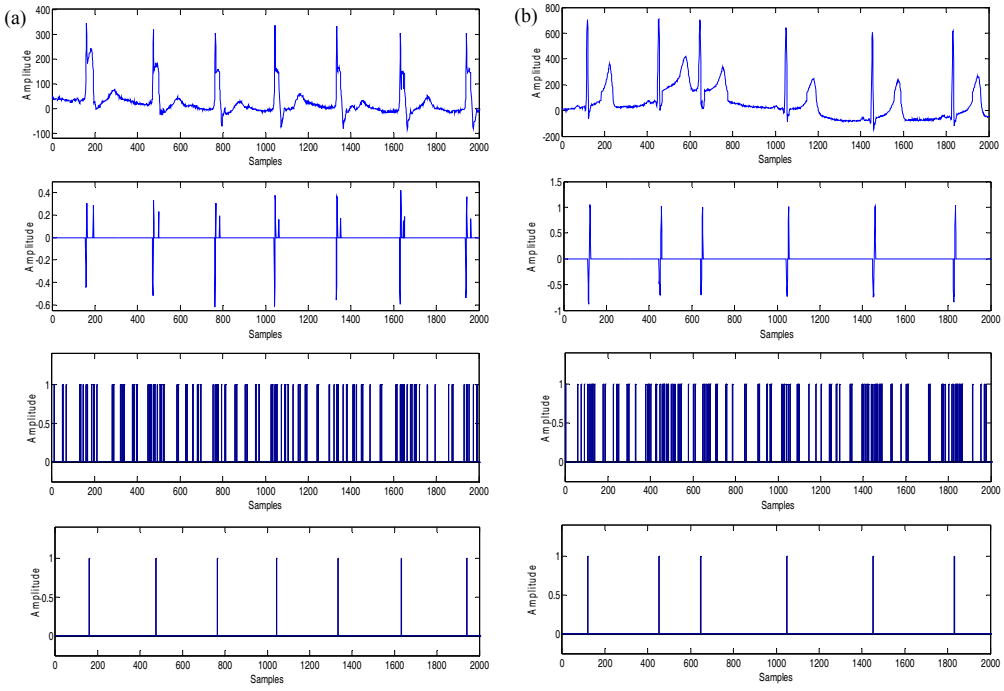

Fig. 7. The *R*-peak detection: above the ECG signal, in the second position the DyWT of the order 3, below the DCM and at the bottom the location of *R* peaks, of the records 102 for (a) and 113 for (b) of the MIT-BIH database

Table 3

Comparison of results with those of various detection algorithms

Detection Algorithm	Total Beats Number	TP	FP	FN	Se	P_+	Failed Detect. (%)	Detect. Accuracy (%)
Our algorithm	33539	33510	12	17	99.95	99.96	0.09	99.91
Yeh *et al*. [27]	33539	33509	22	8	99.98	99.93	0.09	99.91
Adnane *et al*. [28]	33539	33513	23	3	99.99	99.93	0.08	99.92

3.3. R-peak detection. Once we have located all the possible QRS complexes, we must now remove the redundant and isolated pairs. The main idea is to eliminate from two minima (or maxima) the minimum (or maximum) that is the farthest from the maximum (or minimum) of the pair, to have finally the negative minimum-positive maximum pair that are the nearest and which are most likely to be the wavelet transforms of the QRS complex. Then eliminate isolated negative minima-positive maxima pairs and those that are between two real QRS complexes. This is achieved by the removal of pairs that are at a distance less than 0.45 times the mean of three random *RR* intervals. At the end of this stage, we will have a set of negative minima-positive maxima pairs representing the QRS complexes. Since the peak of each complex or the *R* peak is situated between a negative minimum and a positive maximum, we therefore limit the search of the *R* peak in this interval.

Finally, we detect *R* peaks of different QRS complexes from the intervals limited by negative minima-positive maxima pairs. For that, we use the DCM method. We are in the presence of an *R* wave if the DCM is not equal to zero (i.e., DCM = 1).

Actually, we carry out a pretreatment before applying our detection algorithm. The ECG signal filtering by the low and high frequency filters helps to have a more accurate detection due to the removal of the baseline and high frequency noise that may distort the detection operation (Fig. 6).

4. Results

Our wavelet-based detection algorithm was applied to fifteen MIT-BIH database records of 30 minutes each. Few records (numbered from 100 to 124) have been selected randomly from selected patients and the other (numbered 200 to 234) contain plots with major arrhythmic events. Most records were obtained by the modified derivation *D*II by placing the electrodes on the chest; in the others, precordial leads *V*1 and sometimes *V*2 or *V*5 were used [26]. We can check from Fig. 7 (102 and 113 records of the MIT-BIH database), the effectiveness of our algorithm to detect *R* peaks regardless of their types and of their different

rates. Table 2 shows the evaluation results of our algorithm using the false detection rate, computed from the false detections of QRS complexes. These false detections are the sum of false positive detections (*FP*) and false negative detections (*FN*). The *FP* represents the number of *R* peaks detected by the algorithm, whereas they do not exist in the records. The *FN* represents the number of *R* peaks that exist but are not detected by our algorithm. It is noted from the previous table that the detection results are very satisfactory, given a rate of total false detections equal to 0.09 %. Our detection algorithm based on wavelet transforms makes a true *R* wave detection rate equal to 99.91 %, despite the existence of different types of waves and anomalies in the records that may distort the detection.

Our detection results were compared with those in the literature to better position our algorithm in relation with other works on the *R* wave detection of ECG signal. Table 3 compares our results with those of various detections algorithms by choosing the following parameters: the false detection rate, the accuracy detection rates, the sensitivity (*Se*) calculated by (17) and defined by how the method is able to detect true beats, and the positive predictivity (P_+) which is defined as the ability of the method to discriminate false beats from the true ones (18):

$$Se = TP/(TP + FN) \tag{17}$$

$$P_+ = TP/(TP + FP) \tag{18}$$

5. Discussion

From the preceding results, we can state the following remarks:

1) Our detection results, compared with those of the literature [27, 28] (table 3), show that our failed detection ratio is very close to the ratios of the other methods, and it is also true for the comparison of our sensitivity (*Se*) and positive predictivity (P_+) values (equal to 99.95 and 99.96 percent, respectively), which shows the ability of the algorithm to detect true peaks and to eliminate the false ones.
2) Our method is very efficient in terms of precision of *R* peaks location, if we compare it with the method of Li *et al*. in [14] based on wavelet transform (WT) that detects *R* waves as the zero crossing of the WT. The latter method is efficient if there is no deformation of the baseline, but if so, there will be a shift in the location because of the zero line moving.
3) The speed of our method appears in comparison with the same method of Li *et al*. in [14] which uses the wavelet transform at different levels but our detection algorithm is based on a single order (2^3) to locate the QRS complexes. In addition, we conduct this localization by a threshold for the

negative minimum and another for the positive maximum, so we can detect the real QRS complex and not other waves, in contrary to the method in [14] which uses a single threshold for the same pair of negative minimum–positive maximum.

4) Our method is also fast when compared to Xue *et al*. algorithm [11] based on neural networks that takes an enormous time in the learning phase.

5) The complexity analysis is used to estimate the performance of our algorithm compared with those of Yeh *et al.* [27] which uses a difference operation method and Adnane *et al.* [28] that uses three thresholds in the decision stage to compare three signal transformations (squared, normalized and differenced signals). Here, the computational complexity is mainly evaluated in terms of real-valued multiplications, divisions and different iteration steps required for implementing each algorithm. Additions, subtractions and assignment statements are neglected because they are much quicker in most hardware platforms. The complexity of our algorithm is calculated in two steps; the location of QRS complexes by dyadic wavelet transform method and the detection of *R* peaks using DCM method, and it is O(*N*) (i.e., order *N* or greater where *N* is the samples number). However, in [28], an interval of searching *R* peaks is applied on each candidate peak. This additional step will increase the complexity of the algorithm by searching each time in an interval of length *M*, thus, the calculated complexity of this method is O(*M*)+O(*N*), the *N* term is due to different operations (multiplication, thresholding, etc.). The *R*-peak searching window is also used in [27], in addition to O($N\log_2 N$) term due to the use of a spectral representation when performing low-frequency filtering; so the total complexity of this algorithm is O(*M*)+O($N\log_2 N$). We can conclude from this complexity study that our algorithm is faster in its execution compared with the two other methods where a search subset is applied and additionally for the method in [27], the algorithm has O($\log_2 N$) of operations value increase in the complexity of calculation.

6. Conclusion

It was developed in this paper, a new method for detecting *R* waves of electrocardiogram signal based on the dyadic wavelet transform and direction change mark method. This algorithm has given good performance in terms of the accuracy of the location of the QRS complex on the one hand, and in terms of the simplicity of the mathematical calculations used and the speed of execution on the other. However, the artifacts that exist in few records such as records 219 and 230 have distorted the detection of true *R* peaks, despite the use of the filtering unit in the pretreatment step.

R E F E R E N C E S

[1] *D. Jennings, A. Flint, B. C. H. Firton and L. D. M*. Nokes, Introduction to Medical Electronics Applications, Hodder Headline PLC, 1995.

[2] *G. M. Friesen, T. C. Jannett, M.A. Jadallah, S. L. Yates, H. T. Nagle*, "A comparison of the noise sensitivity of nine QRS detection algorithms", IEEE Transactions on Biomedical Engineering, **vol. 37**, pp. 85-98, Jan. 1990.

[3] *Y. C. Yeha, W. J. Wang*, "QRS complexes detection for ECG signal: the difference operation method", Computer Methods and Programs in Biomedicine, **vol. 91**, pp. 245–254, Apr. 2008.

[4] *J. Pan, W. J. Tompkins*, "A real time QRS detection algorithm", IEEE Transactions on Biomedical Engineering, **vol. BME-32**, pp. 230-236, Mar. 1985.

[5] *M. Kunt, H. Rey, A. Lingtenberg*, "Preprocessing of electrocardiograms by digital techniques", North-Holland Publishing Company, **vol. 4**, pp. 215-222, Apr. 1982.

[6] *M. Adnane, Z. Jiang, S. Choi*, "Development of QRS detection algorithm designed for wearable cardiorespiratory system," Computer Methods and Programs in Biomedicine, **vol. 93**, pp. 20-31, Jul. 2009.

[7] *S. W. Chena, H. C. Chena, H. L. Chan*, "A real-time QRS detection method based on moving-averaging incorporating with wavelet denoising", Computer Methods and Programs in Biomedicine, **vol. 82**, pp. 187-195, Nov. 2006.

[8] *F. Portet*, Pilotage d'Algorithmes pour la Reconnaissance en Ligne d'Arythmies Cardiaques, Thesis, University of Renne, 2005.

[9] *J. S. Paul, M. R. Reddy, V. J. Kumar*, "A QRS estimator using linear prediction approach", Signal Processing, **vol. 72**, 15-22, Jan. 1999.

[10] *K. P. Li, W. H. Chang*, "QRS feature extraction using linear prediction", IEEE Transactions on Biomedical Engineering, **vol. 36**, pp. 1050-1055, Oct. 1989.

[11] *Q. Xue, Y. H. Hu, W. J. Tompkins*, "Neural-network-based adaptive matched filtering for QRS detection", IEEE Transactions on Biomedical Engineering, **vol. 39**, pp. 317-329, Apr. 1992.

[12] *A. De Gaetano, S. Panunzi, F. Rinaldi, A. Risi, M. Sciandrone*, "A patient adaptable ECG beat classifier based on neural networks", Applied Mathematics and Computation, **vol. 213**, pp. 243-249, Jul. 2009.

[13] *V. X. Alfonso, W. J. Tompkins, T. Q. Nguyen, S. Luo*, "Multirate processing of the ECG using filter banks", IEEE Computers in Cardiology, **vol. 149**, pp. 245-248, Sep. 1996.

[14] *C. Li, C. Zheng, C.Tai*, "Detection of ECG characteristic points using wavelet transforms," IEEE Transactions on Biomedical Engineering, **vol. 42**, pp. 21-28, Jan. 1995.

[15] *C. H. Lin, Y. C. Du, T. Chen*, "Adaptive wavelet network for multiple cardiac arrhythmias recognition", Expert Systems with Applications, **vol. 34**, pp. 2601-2611, May 2008.

[16] *J. S. Sahambi, S. N. Tandon, R. K. P. Bhatt*, "Using wavelet transforms for ECG characterization", IEEE Engineering, Medicine and Biology, **vol. 16**, pp. 77-83, Jan./Feb. 1997.

[17] *P. J. M. Fard, M. H. Moradi, M. R. Tajvidi*, "A novel approach in R peak detection using hybrid complex wavelet (HCW)", International Journal of Cardiology, **vol. 124**, pp. 250-253, Feb. 2008.

[18] *S. Kadambe, R. Murray, F. Boudreaux-Bartels*, "Wavelet transform-based QRS complex detector", IEEE Transactions on Biomedical Engineering, **vol. 46**, pp. 838-848, Jul. 1999.

[19] *J. P. Martínez, R. Almeida, S. Olmos, A. P. Rocha, P. Laguna*, "A wavelet-based ECG delineator: evaluation on standard databases", IEEE Transactions on Biomedical Engineering, **vol. 51**, pp. 570-581, Apr. 2004.

[20] *J. P. V. Madeiro, P. C. Cortez, F. I. Oliveira, R. S. Siqueira*, "A new approach to QRS segmentation based on wavelet bases and adaptive threshold technique", Medical Engineering and Physics, **vol. 29**, pp. 26-37, Jan. 2007.
[21] *A. Ghaffari, H. Golbayani, M. Ghasemi*, "A new mathematical based QRS detector using continuous wavelet transform," Computers and Electrical Engineering, **vol. 34**, pp. 81-91, Mar. 2008.
[22] *S. Mallat*, A Wavelet, Tour of Signal Processing, Elsevier, 1998.
[23] *R. X. Gao, R. Yan*, Wavelets Theory and Applications for Manufacturing, Springer, 2011.
[24] *J. C. Goswami, A. Chan*, Fundamentals of Wavelets: Theory, Algorithms and Applications, Wiley, 2011.
[25] *A. Khawaja*, Automatic ECG Analysis using Principal Component Analysis and Wavelet Transformation, Karlsruhe Transactions on Biomedical Engineering, **vol. 3**, 2007.
[26] *G. B. Moody*, ECG Database Applications Guide, Harvard University, 1992.
[27] *Y. C. Yeh, W. J. Wang*, "QRS complexes detection for ECG signal: the difference operation method", Computer Methods and Programs in Biomedicine, **vol. 91**, pp. 245-254, Apr. 2008.
[28] *M. Adnane, Z. Jiang, S. Choi*, "Development of QRS detection algorithm designed for wearable cardiorespiratory system", Computer Methods and Programs in Biomedicine, **vol. 03**, pp. 20-31, Jul. 2009.